

## A kinetic study of the thermal degradation of cetyltrimethylammonium bromide inside the mesoporous SBA-3 molecular sieve

DJORDJE STOJAKOVIĆ<sup>1\*</sup>, NEVENKA RAJIĆ<sup>1</sup>, MAJA MRAK<sup>2</sup> and  
VENČESLAV KAUČIČ<sup>3</sup>

<sup>1</sup>Faculty of Technology and Metallurgy, University of Belgrade, 11000 Belgrade, Serbia,

<sup>2</sup>Jožef Štefan Institute, Jamova 39, 1000 Ljubljana and <sup>3</sup>National Institute of Chemistry, Hajdrihova 19, 1000 Ljubljana, Slovenia

(Received 12 June 2007)

**Abstract:** The thermal degradation of cetyltrimethylammonium bromide (CTMAB) inside the mesoporous SBA-3 was studied under non-isothermal conditions. There are two distinct and complex kinetic processes which partly overlap, each consisting of one dominant and three minor individual processes. The two dominant processes can be described by the Sestak–Berggren model. The main decomposition step (the first dominant process) involves the overcoming of weak interactions between CTMAB and the silica network and proceeds with a lower  $E_a$  value ( $116 \pm 2$  kJ mol<sup>-1</sup>) than the second dominant process ( $153 \pm 5$  kJ mol<sup>-1</sup>), which can be explained by the size reduction of the pore openings due to the contraction of the SBA-3 unit cell caused by the removal of CTMAB.

**Keywords:** NPK method, non-isothermal kinetics, open-framework, SBA-3, cetyltrimethylammonium bromide (CTMAB).

### INTRODUCTION

Microporous inorganic solids having pore diameters less than 2 nm and mesoporous inorganic solids with pore diameters ranging from 2 to 50 nm are of great industrial importance since they exhibit unique catalytic and sorption properties. This is mainly caused by their large internal surface area.

Microporous solids are generally prepared under hydrothermal conditions using different amines and/or quaternary amine salts which play a crucial structure-directing role.<sup>1</sup> Mesoporous materials are usually obtained by a liquid-crystal template mechanism (LCT) using mostly alkyltrimethylammonium surfactants. In the LCT mechanism, the inorganic phase occupies the continuous water (solvent) region to create inorganic walls between ordered surfactant micelles.<sup>2</sup>

\* Corresponding author. E-mail: stojakovic@tmf.bg.ac.yu  
doi: 10.2298/JSC0712309S

The as-synthesized mesoporous solid contains more than 50 % organic material by weight and is in effect an organic-inorganic composite.

An efficient removal of the organic component from the as-synthesized solid in order to access the internal free space is an important step in the final preparation of the porous materials. Recently, kinetic studies of the removal of cetyltrimethylammonium bromide (CTMAB) from MCM-41 and MCM-48 siliceous materials have been reported.<sup>3,4</sup> Both solids belong to the type having cubic mesostructured frameworks. It was found that the activation energy for the removal of CTMAB species from MCM-41 is rather high, having a value of  $166 \pm 8.2 \text{ kJ mol}^{-1}$ .<sup>3</sup> The removal of CTMAB from MCM-48 proceeds with an even higher activation energy ( $178 \pm 8.5 \text{ kJ mol}^{-1}$ ).<sup>4</sup>

In this study, the thermal removal of CTMAB from SBA-3 solid was examined. The latter is mesoporous silica having a pore size ranging from 2.2 to 2.5 nm.<sup>5</sup> In contrast to the syntheses of MCM-41 and MCM-48, which are performed in alkaline conditions, the preparation of SBA-3 proceeds in a strongly acidic solution below the isoelectric point of silica. During the polymerization process, the protons bound to silica species are eliminated, leaving the inorganic phase of the SBA-3 product electrically neutral. In contrast, the MCM materials obtained under alkaline conditions have a negatively charged silica network.<sup>6</sup> As the SBA-3 network is electrically neutral, it is to be expected that the main factor in the removal of CTMAB from SBA-3 would involve the overcoming of the framework-surfactant non-bonded interactions.

The kinetics of the thermal removal (decomposition) of CTMAB has been studied by the non-parametric kinetics (NPK) method of Serra *et al.*<sup>7-9</sup> The NPK method has been applied in recent years for the kinetic analysis of thermal degradation in a variety of chemical systems, *e.g.*, bis-urethanes,<sup>10</sup> transition metal carboxylates,<sup>11</sup> alkaline metal phosphates<sup>12</sup> and glutamates,<sup>13</sup> alkaline metal and alkaline-earth metal benzoates,<sup>13</sup> and a 3-D zincophosphate containing occluded ammonium species.<sup>14</sup>

## EXPERIMENTAL

### *Synthesis*

Cetyltrimethylammonium bromide (CTMAB, Aldrich) and tetraethyl orthosilicate (TEOS, Aldrich, 98 wt. %) were used as the surfactant and the silica source, respectively. The following molar composition of reactants was used:  $\text{SiO}_2:4.9\text{HCl}:0.24\text{CTMAB}:147\text{H}_2\text{O}$ . The CTMAB was dissolved in dilute hydrochloric acid ( $\approx 1.8 \text{ mol dm}^{-3}$ ) and then TEOS was added. The resulting mixture was stirred for about 2 h at room temperature and then aged without stirring for the next 72 h. The resultant white solid (SBA-3) was washed with deionized water and dried at 60 °C overnight. The mesostructure of SBA-3<sup>5</sup> was confirmed by the powder X-ray diffraction method [three diffractions at  $2\theta = 2.7, 4.7$  and  $5.3^\circ$  are evident in the XRD pattern (recorded using  $\text{CuK}\alpha$  radiation)]. The scanning electron micrograph (Fig. 1) reveals particles with a shape resembling interconnected snail shells.

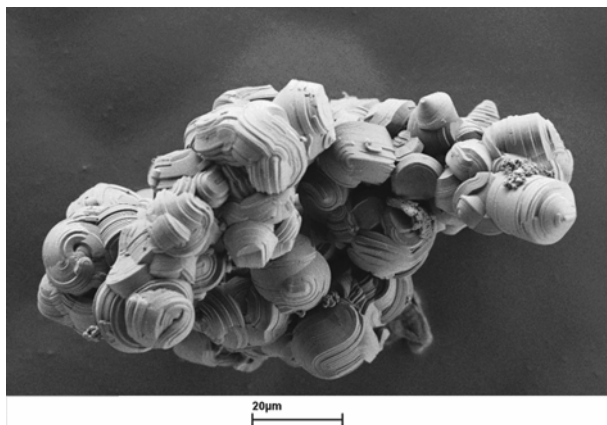


Fig. 1. SEM microphotograph of the as-synthesized SBA-3.

#### Instrumentation

The thermal decomposition measurements were performed using a SDT Q-600 simultaneous DSC–TGA instrument (TA Instruments). The samples (mass approx. 10 mg) were heated in a standard 90  $\mu\text{l}$  alumina sample pan. All experiments were carried out under dynamic air at a flow rate of 0.1  $\text{dm}^3 \text{min}^{-1}$ . Non-isothermal measurements were conducted at heating rates of 3, 6, 9, 12, and 16  $\text{K min}^{-1}$ . Five experiments were performed at each heating rate.

#### RESULTS AND DISCUSSION

The TG and DTG curves for SBA-3 in the 300–1050 K range are shown in Fig. 2. The profiles of TG–DTA curves do not significantly differ from those of the MCM materials.<sup>3,4,6</sup> There are three main weight losses, two of them being sharp and distinct. The first loss (40 %) occurs in the 470–593 K range and it is centered at 519 K. The second weight loss (7.5 %, centered at 620 K) occurs in the 593–665 K range. The third loss (8.5 %) is rather diffuse-looking since it proceeds over a broad temperature range (670–950 K). The overall mass loss amounts to about 56 %, which is in accordance with the C,H,N-analysis of SBA-3.

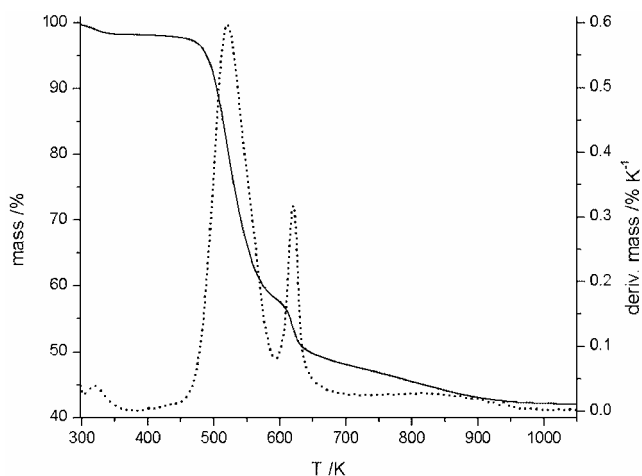


Fig. 2. TG/DTG curves for SBA-3 (TG: solid line; DTG: dotted line).

The first and second weight losses correspond to the decomposition of the surfactant, whereas the third loss can be attributed to the oxidative removal of residual carbonaceous species and the condensation of the remaining silanol groups.<sup>3,4,6</sup>

#### *Kinetics of CTMAB decomposition during the thermal treatment of SBA-3*

The decomposition of CTMAB during thermal treatment of SBA-3 was studied in an oxidative atmosphere under non-isothermal conditions. The measurements were performed at five different heating rates ( $\beta$ ): 3, 6, 9, 12 and 16 K min<sup>-1</sup>. The degrees of conversion,  $\alpha$ , vs. the absolute temperature,  $T$ , thermogravimetry curves are shown in Fig. 3 and the corresponding reaction rates are shown in Fig. 4.

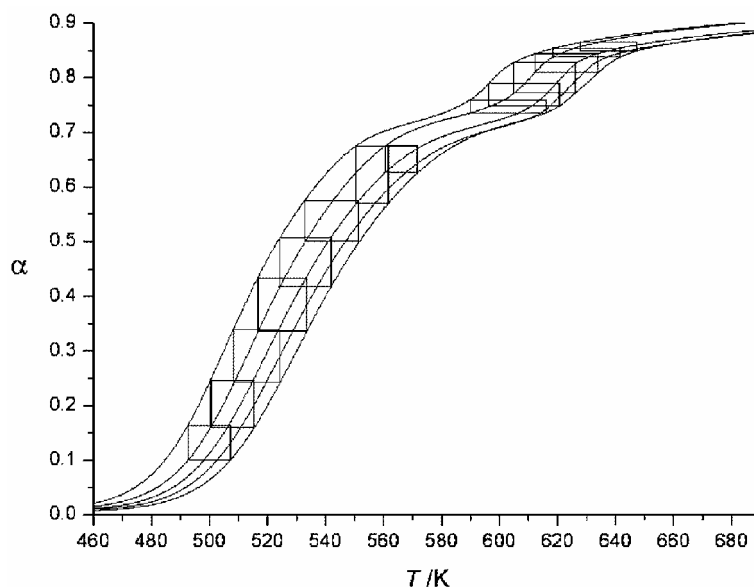


Fig. 3. Experimental curves for the decomposition of CTMAB in SBA-3 at different heating rates (from left to right: 3, 6, 9, 12 and 16 °C min<sup>-1</sup>). The rectangles show the submatrices selected for the NPK analysis.

The kinetics of the decomposition of CTMAB were examined by the NPK method.<sup>7-9,15</sup> This method for the analysis of non-isothermal thermogravimetry data is based on the usual assumption that the reaction rate can be expressed as the product of two independent functions,  $f(\alpha)$  and  $h(T)$ , where  $f(\alpha)$  accounts for the kinetic model while  $h(T)$  is a temperature-dependent function, usually the Arrhenius equation:

$$h(T) = k = A \exp(-E_a/RT)$$

The reaction rates,  $d\alpha/dt$ , measured from several experiments at different heating rates, can be expressed as a three-dimensional surface determined by the temperature and the degree of conversion. This surface can be organized as an ( $n \times m$ )

matrix  $A$ , in which the rows correspond to different degrees of conversion, from  $\alpha_1$  to  $\alpha_n$ , while the columns correspond to different temperatures, from  $T_1$  to  $T_m$ .

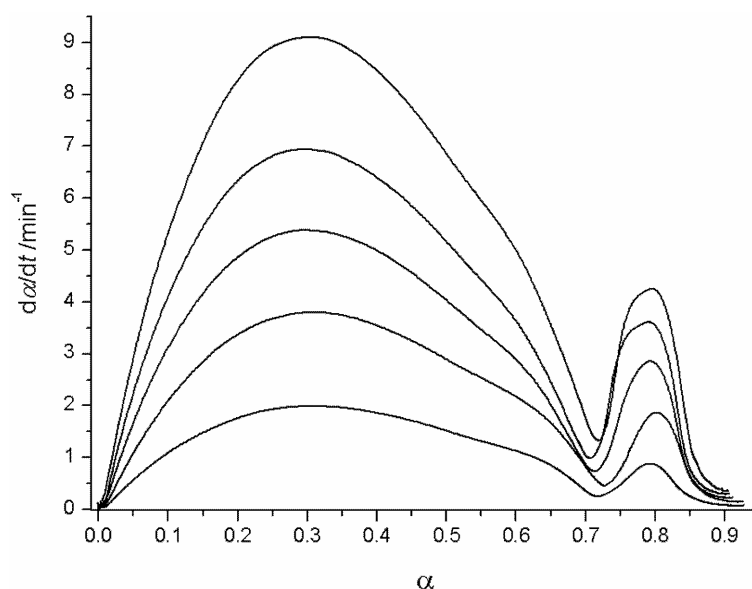


Fig. 4. Experimental reaction rates vs. the degree of conversion for the decomposition of CTMAB in SBA-3 at different heating rates (from bottom to top: 3, 6, 9, 12 and 16 °C min<sup>-1</sup>).

The reaction rate, *i.e.*, the matrix  $A$ , can be expressed as the product of two vectors:

$$A = fh^T$$

where

$$f^T = [f(\alpha_1) f(\alpha_2) f(\alpha_3) \dots f(\alpha_n)]$$

$$h^T = [h(T_1) h(T_2) h(T_3) \dots h(T_m)]$$

In the next step of the NPK method, the matrix  $A$  is decomposed in order to obtain the vectors  $f$  and  $h$ . This is done by the mathematical procedure known as the singular value decomposition (SVD). From the vectors  $f$  and  $h$ , plots of  $f(\alpha)$  against  $\alpha$  and of  $h(T)$  against  $T$  are readily available and the nature of the functions  $f(\alpha)$  and  $h(T)$  can be examined. This is a model-free method since it yields the temperature dependence of the reaction rate without having to make any prior assumptions about the kinetic model.

In actual practice, it is not possible to experimentally obtain all the elements of the matrix  $A$  for a sufficient range of alpha values and temperatures. Therefore, the  $\alpha$  vs.  $T$  curves are divided into partly overlapping submatrices. SVD is then applied to each submatrix; if  $q$  submatrices were formed, the SVD on each of them will yield  $q$  matrices  $U_i$  and  $V_i$  as well as  $q$  singular value vectors  $s_i$ ,

respectively. Finally, from the vectors  $u_i$  and  $v_i$  of the individual matrices  $U_i$  and  $V_i$ , the continuous vectors  $u$  and  $v$  can be obtained.<sup>8,16,17</sup> The results contained in the vector  $u$  are proportional to the function of conversion,  $f(\alpha)$ , and those in the vector  $v$  are proportional to the function of temperature,  $h(T)$ .

Fig. 4 confirms the observation stated in referring to Fig. 2, namely that the decomposition of CTMAB occurs in two distinct and fairly well separated main processes. The first one (process I) takes place approximately in the  $\alpha$  range of 0.0–0.78, and the second one (process II) in the  $\alpha$  range 0.67–0.9; there is a partial overlap of the two processes in the  $\alpha$  region 0.67–0.78. The third mass loss (very broad) visible in Fig. 2 lies in the  $\alpha$  region ranging from about 0.86 to 1 and it partly overlaps with process II. The NPK analysis was performed separately for process I and process II in the appropriate  $\alpha$  regions. The third process could not be kinetically analyzed due to the large breadth of its temperature range.

#### *Process I*

The NPK treatment of the thermogravimetry data yielded 8 submatrices in the alpha range 0.1–0.68 and the temperature range of 493–572 K (Fig. 3); a total of 32 different alpha values and 28 different temperatures were used for the construction of the 8 submatrices. After SVD had been applied on each submatrix, the resulting  $s_i$  vectors contained in all 8 cases one dominant value and three smaller values. In particular, for the first six submatrices, the dominant value in each individual  $s_i$  accounts for more than 96 % of the sum of the values of this vector, whereas the other three values amount to approximately 2 %, 1 %, and 0.1 %, respectively. For the seventh and eighth submatrix, the dominant value accounts for about 93 %, and the other three for 5.4, 1.4, and 0.2 %, respectively. This indicates that in the 493–572 K temperature range there is one dominant kinetic process (process I-1), accompanied by three minor processes (processes I-2, I-3 and I-4).

Further kinetic analysis of process I was performed only for the dominant process I-1. The remaining three minor processes were not examined for the following reason. When more than one kinetic process is present, the individual vectors  $u$  for each process are in effect some linear combination of the corresponding true “kinetic vectors”.<sup>18</sup> In the same manner, the individual vectors  $v$  are also the result of a linear combination. These linear combinations can be broken down only if the kinetic model for each of the processes is known. If these models are not known, it seems meaningful to analyze vectors  $u$  and  $v$  only for the process which is markedly predominant (provided one exists). Namely, in such circumstances one can reasonably assume that the vectors  $u$  and  $v$  of the dominant process should not differ significantly from the “kinetic vectors”, whereas the corresponding vectors of the minor processes will be heavily influenced by the linear combination.

The kinetic analysis for the process I-1 proceeded as follows. From the vectors  $u_i$  and  $v_i$  of the individual matrices  $U_i$  and  $V_i$  the continuous vectors for the process I-1,  $u_1$  and  $v_1$ , were compiled. Fig. 5 shows the plot of the  $f(\alpha)$  values from the vector  $u_1$  vs.  $\alpha$ . The  $\alpha_1$  scale in Fig. 5 was obtained by rescaling the experimental  $\alpha$  range (0.0–0.78) which fully encompasses process I into an  $\alpha$  range of 0.0–1.0. The  $f(\alpha)$  values were examined against various known kinetic models, but the vector  $u_1$  could not be satisfactorily fitted in most of them ( $R^2$  of the fits being invariably  $< 0.9$ ). Only the Sestak–Berggren model<sup>19</sup> yielded acceptable fits, the best fit (Fig. 5) being obtained with the two parameter Sestak–Berggren Eq. (1). The obtained parameters are  $m = -0.157 \pm 0.006$  and  $n = 1.98 \pm 0.03$ , with  $R^2 = 0.997$ .

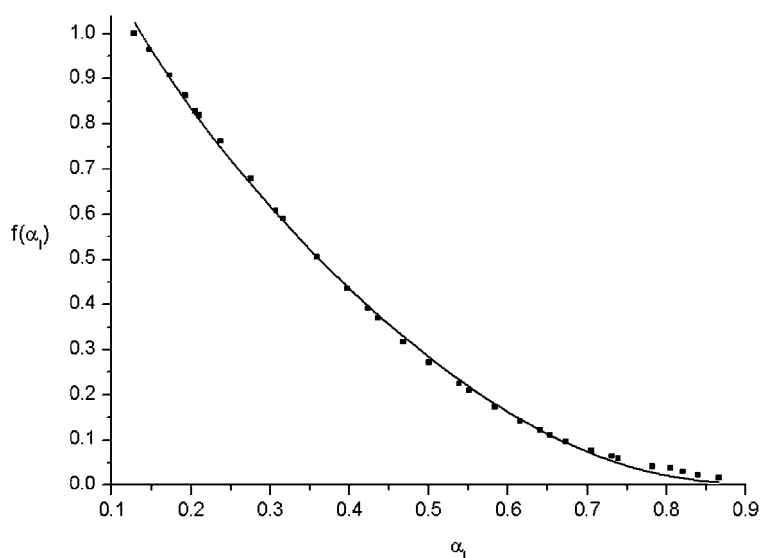


Fig 5. A plot of  $f(\alpha)$  [normalized within (0,1)] vs. the rescaled degree of conversion for the process I-1: dark squares are the experimental points, while the line is the fit obtained by Eq. (2).

$$f(\alpha) = \alpha^m(1 - \alpha)^n \quad (1)$$

$$f(\alpha) = \alpha^{-0.157}(1 - \alpha)^{1.98} \quad (2)$$

It is worth noticing that the resulting Eq. (2) is a valid kinetic expression in the sense that it fulfils two boundary conditions<sup>20</sup> which a function must satisfy in order to consistently represent a given kinetic model. The two conditions are:

$$\lim_{\alpha \rightarrow 0} g(\alpha) = 0$$

and

$$\lim_{\alpha \rightarrow 1} g(\alpha) = \infty$$

where  $g(\alpha)$  is the integrated form of  $f(\alpha)$ .

The plot of the  $\ln [h(T)]$  values from the compiled vector  $v_1$  vs.  $1/T$  is shown in Fig. 6. The slope of the straight line ( $R = 0.997$ ) gives the activation energy as  $E_a = 116 \pm 2 \text{ kJ mol}^{-1}$ . From the intercept, the value of  $(5.6 \pm 2) \times 10^{12} \text{ min}^{-1}$  is obtained and it essentially represents the Arrhenius pre-exponential constant  $A$ , somewhat modified by constants arising from scaling.<sup>16</sup>

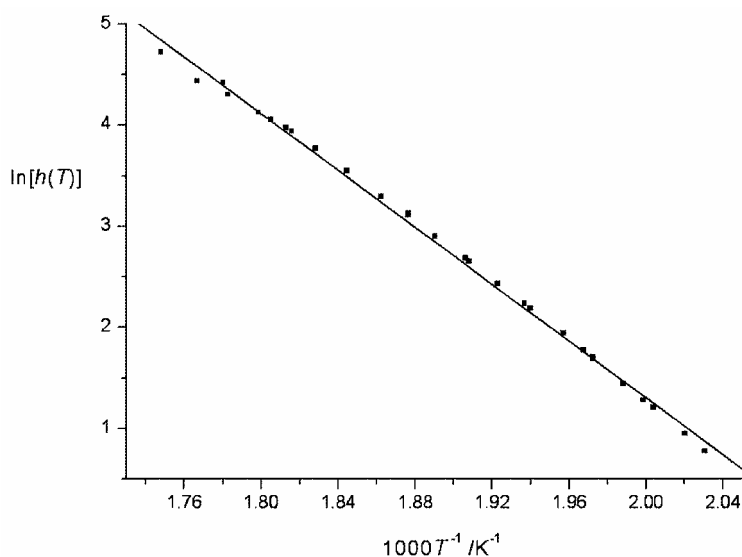


Fig. 6. An Arrhenius plot of  $\ln [h(T)]$  vs.  $1/T$  for the process I-1: the squares are the experimental points and the straight line is the best fit.

The relatively low  $E_a$  value for the process I-1 reflects the fact that a major factor influencing the removal of CTMAB from siliceous networks is the strength of the CTMAB-framework interactions. The framework-surfactant interactions in SBA-3 are not very strong since the inorganic framework is electrically neutral.

The obtained  $E_a$  value for process I-1 can be compared with the  $E_a$  values of 166 and 178  $\text{kJ mol}^{-1}$  found for the thermal removal of CTMAB from MCM-41 and MCM-48 materials, respectively.<sup>3,4</sup> It is not surprising that these two values are higher than the  $E_a$  value obtained for SBA-3 since the mesoporous network of the MCM materials is based on stronger cooperative electrostatic interactions between negatively charged oligomeric silicate species and positively charged CTMA<sup>+</sup> ions.<sup>21</sup> The relatively weak intermolecular-type interactions in the SBA-3 framework allow CTMAB to be removed more easily than from MCM materials and this is essentially reflected in the corresponding activation energies.

### Process II

The NPK treatment of the thermogravimetry data yielded 6 submatrices in the alpha range of 0.73–0.86 and the temperature range of 593–648 K (Fig. 3); a

total of 25 different  $\alpha$  values and 24 different temperatures were used for the construction of 6 submatrices. After SVD had been applied on each submatrix, the resulting  $s_i$  vectors contained in all 6 cases one dominant value and three smaller values. In particular, for the first four submatrices the dominant value in each individual  $s_i$  accounts for more than 92 % of the sum of values of this vector, whereas the other three values amount to approximately 4, 2.5 and 0.2 %, respectively. For the fifth and sixth submatrix, the dominant value accounts for about 84 % and the other three for 11, 4 and 0.9 %, respectively. This indicates that there is one major kinetic process (process II-1), together with three minor processes (processes II-2, II-3 and II-4) in the 588–648 K temperature range.

For the same reason as given for process I, further kinetic analysis of process II was performed only for process II-1, in an analogous manner as for process I-1.

The plot of the  $f(\alpha)$  values from the vector  $u_1$  vs.  $\alpha$  is shown in Fig. 7. The  $\alpha_{II}$  scale in Fig. 7 was obtained by rescaling the experimental  $\alpha$  range of 0.66–0.9 (which essentially encompasses the entire process II) into an  $\alpha$  range of 0.0–1.0. The  $f(\alpha)$  values for process II-1 could be satisfactorily fitted only with the empirical three-parameter Sestak–Berggren Eq. (3); which gives a fit having  $R^2 = 0.994$ , with the parameters  $m = -116 \pm 0.9$ ,  $n = 55 \pm 0.4$  and  $p = 116 \pm 0.8$ .

$$f(\alpha) = \alpha^m (1-\alpha)^n (-\ln(1-\alpha))^p \quad (3)$$

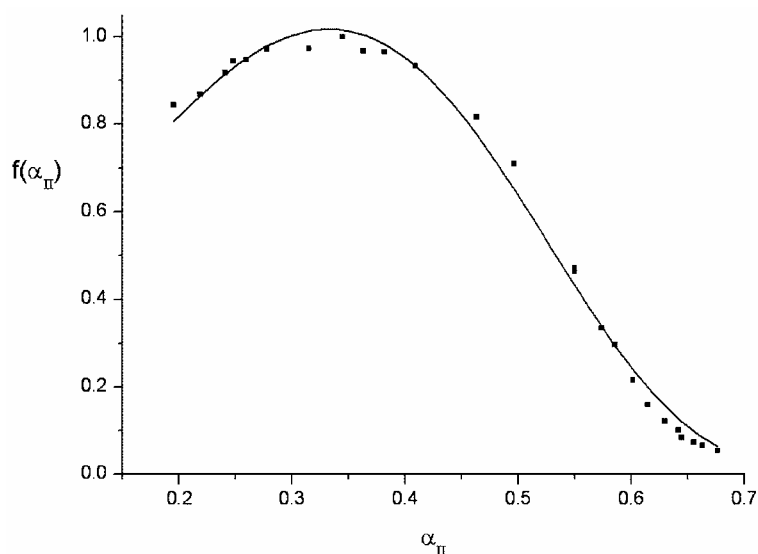


Fig 7. A plot of  $f(\alpha)$  [normalized within (0,1)] vs. the rescaled degree of conversion for the process II-1: dark squares are the experimental points and the line is the fit obtained by Eq. (1).

The plot of the  $\ln[h(T)]$  values from the compiled vector  $v_1$  vs.  $1/T$  is shown in Fig. 8. The slope of the straight line ( $R = 0.989$ ) gives the activation energy as  $E_a = 153 \pm 5 \text{ kJ mol}^{-1}$ . From the intercept, the Arrhenius pre-exponential constant  $A$  is found to be  $(2.3 \pm 2) \times 10^{13} \text{ min}^{-1}$ .

The finding that the  $E_a$  of the process II-1 is higher than that for the process I-1 could be explained by the fact that the removal of CTMAB from SBA-3 causes a significant contraction of the unit cell of the remaining siliceous material (a contraction of approx. 18 %).<sup>6</sup> After the bulk of the CTMAB has been decomposed by the first process, the ensuing contraction of the unit cell renders the removal of the remaining parts of surfactant more difficult due to the reduced size of the pore openings.

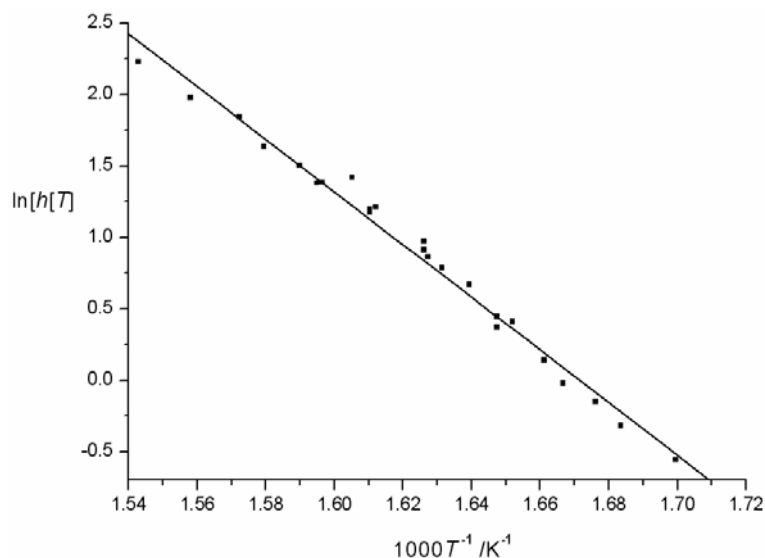


Fig. 8. An Arrhenius plot of  $\ln [h(T)]$  vs.  $1/T$  for the process II-1: the squares are the experimental points and the straight line is the best fit.

#### CONCLUSIONS

The removal of CTMAB from mesostructured SBA-3 was studied under non-isothermal conditions. There are two distinct and complex kinetic processes which partly overlap, each consisting of one dominant and three minor individual processes. Both the dominant processes can be described by the Sestak–Berggren model. The main decomposition step (the first dominant process) proceeds with a rather low  $E_a$  value for this type of system, due to weak intermolecular-type interactions between CTMAB and the silica network. The second decomposition step (the second dominant process) has a higher  $E_a$  value than the first one, indicating that it is primarily controlled by the size of the pore openings.

The non-parametric kinetics method proved helpful in the separate analyzes of the partly overlapping processes.

*Acknowledgements.* This work was supported by the bilateral project “By rational synthesis towards smart materials” financed by the Serbian Ministry of Science and the Slovenian Ministry of Higher Education Science and Technology. The authors also wish to thank Mr. Alen Kljajić for the preparation of the SBA-3 material.

## ИЗВОД

КИНЕТИЧКО ИЗУЧАВАЊЕ ТЕРМИЧКОГ РАЗЛАГАЊА  
ЦЕТИЛТРИМЕТИЛАМОНИЈУМ–БРОМИДА УНУТАР  
МЕЗОПОРОЗНОГ МОЛЕКУЛСКОГ СИТА SBA-3БОРБЕ СТОЈАКОВИЋ<sup>1</sup>, НЕВЕНКА РАЈИЋ<sup>1</sup>, МАЈА МРАК<sup>2</sup> и ВЕНЧЕСЛАВ КАУЧИЋ<sup>3</sup><sup>1</sup>Технолошко–металуршки факултет, Универзитет у Београду, 11000 Београд, Србија, <sup>2</sup>Jožef Štefan Institute, Jamova 39, 1000 Ljubljana и <sup>3</sup>National Institute of Chemistry, Hajdrihova 19, 1000 Ljubljana, Slovenia

Изучавано је термичко разлагање под неизотермским условима цетилтриметиламонијум-бромид (СТМАВ) унутар мезопорозног SBA-3. Постоје два разветна и сложена кинетичка процеса који се делимично преклапају, при чему се оба састоје од по једног преовлађујућег и три споредна индивидуална процеса. Два преовлађујућа процеса могу се описати помоћу Шестак–Бергеновог модела. У главном ступњу разлагања (у првом преовлађујућем процесу) бивају надвладане слабе интеракције између СТМАВ и решетке силицијум-диоксида, и тај ступањ се одвија уз мању вредност  $E_a$  ( $116 \pm 2$  kJ mol<sup>-1</sup>). Другом преовлађујућем процесу одговара већа вредност  $E_a$  ( $153 \pm 5$  kJ mol<sup>-1</sup>) него првом процесу, што се може објаснити смањењем величине отвора пора услед контракције јединичне ћелије SBA-3 изазване уклањањем цетилтриметиламонијум-бромид.

(Примљено 12. јуна 2007)

## REFERENCES

1. N. Rajić, *J. Serb. Chem. Soc.* **70** (2005) 371
2. C. T. Kresge, M. E. Leonowicz, W. J. Roth, J. C. Vartuli, J. S. Beck, *Nature* **359** (1992) 710
3. M. J. B. Souza, A. O. S. Silva, J. M. F. B. Aquino, V. J. Fernandes Jr., A. S. Araujo, *J. Thermal Anal. Cal.* **75** (2004) 693
4. M. J. B. Souza, A. O. S. Silva, J. M. F. B. Aquino, V. J. Fernandes Jr., A. S. Araujo, *J. Thermal Anal. Cal.* **79** (2005) 493
5. F. Chen, S. Shen, X. –J. Xu, R. Xu, F. Kooli, *Microporous Mesoporous Mater.* **79** (2005) 85
6. F. Kleitz, W. Schmidt, F. Schuth, *Microporous Mesoporous Mater.* **65** (2003) 1
7. R. Serra, R. Nomen, J. Sempere, *J. Therm. Anal. Cal.* **52** (1998) 933
8. R. Serra, R. Nomen, J. Sempere, *Thermochim. Acta* **316** (1998) 37
9. J. Sempere, R. Nomen, R. Serra, *J. Therm. Anal. Cal.* **56** (1999) 843
10. T. Vlase, G. Vlase, N. Doca, C. Bolcu, *J. Therm. Anal. Cal.* **80** (2005) 59
11. T. Vlase, G. Vlase, A. Chiriac, N. Doca, *J. Therm. Anal. Cal.* **80** (2005) 87
12. T. Vlase, G. Vlase, N. Doca, *J. Therm. Anal. Cal.* **80** (2005) 207
13. T. Vlase, G. Vlase, N. Doca, *J. Therm. Anal. Cal.* **80** (2005) 425
14. Dj. Stojakovic, N. Rajic, N. Zabukovec Logar, V. Kaucic, *Thermochim. Acta* **449** (2006) 42
15. M. E. Brown, M. Maciejewski, S. Vyazovkin, R. Nomen, J. Sempere, A. Burnham, J. Opfermann, R. Strey, H. L. Anderson, A. Kemmler, R. Keuleers, J. Janssens, H. O. Desseyn, C.-R. Li, T. B. Tang, B. Roduit, J. Malek, T. Mitsuhashi, *Thermochim. Acta* **355** (2000) 125
16. J. D. Sewry, M. E. Brown, *Thermochim. Acta* **390** (2002) 217
17. J. Sempere, R. Nomen, R. Serra, J. Soravilla, *Thermochim. Acta* **388** (2002) 407
18. J. Sempere, R. Nomen, *EU01-18 – Non-Parametric Kinetics (NPK) – Can it be used in Reaction Calorimetry?*, 10<sup>th</sup> RXE User Forum Europe, Lucerne, Switzerland, November 2001, [http://us.mt.com/mt/appEdStyle/wr\\_RXEForum\\_EU01\\_18\\_Editorial-Generic\\_1117531464103.jsp](http://us.mt.com/mt/appEdStyle/wr_RXEForum_EU01_18_Editorial-Generic_1117531464103.jsp), (April 16, 2007)
19. J. Sestak, G. Berggren, *Thermochim. Acta* **3** (1971) 1
20. J. Malek, J. M. Criado, J. Sestak, J. Militky, *Thermochim. Acta* **153** (1989) 429
21. R. Zana, J. Frasch, M. Soulard, B. Lebeau, J. Patarin, *Langmuir* **15** (1999) 2603.